

## Nanometer Scale Characterization of Polymer Films by Atomic-Force Microscopy

Christian Teichert<sup>1</sup>\*, Alfred Haas<sup>1</sup>, Gernot M. Wallner<sup>2</sup>, Reinhold W. Lang<sup>2</sup>

<sup>1</sup>Institute of Physics, University of Leoben, Franz-Josef-Str. 18,  
A-8700 Leoben, Austria

<sup>2</sup>Institute of Materials Science and Testing of Plastics, University of Leoben,  
Franz-Josef-Str. 18, A-8700 Leoben, Austria

**Summary:** Atomic-force microscopy was applied to perform a comprehensive surface roughness characterization of commercially available, highly transparent polymer films for transparent insulation applications. The morphological characterization included evaluation of the root-mean-square roughness, the lateral correlation length of roughness as well as the roughness exponent. In addition, high-resolution scans have been recorded yielding morphological information on a length scale of only a few ten nm. These measurements revealed the correlation between surface nanostructure and fabrication technique. For an impact-modified polymethylmethacrylate film with rubber inclusions phase images clearly uncovered the core-shell structure of these inclusions.

### Introduction

Polymer films are widely used for products in active and passive solar energy utilization, e.g., as embedding material in photovoltaic cells or as structure material for transparent heat insulation. In this respect, their solar optical properties play an important role. Especially for highly transparent films, these properties are substantially determined by the film surface. A systematic investigation of the optical properties in the solar and infrared wavelength range of commercially available polymer films for transparent heat insulation indicated the existence of surface structures with lateral dimensions of less than 300 nm.<sup>[1]</sup> These results motivated the application of atomic-force microscopy (AFM) that allows a quantitative characterization of the surface morphology down to the nanometer scale. For a representative collection of amorphous and semi-crystalline polymer films comprising polycarbonate (PC), polymethylmethacrylate (PMMA), cellulose acetate (CA, two different CA films have been investigated called hereafter CA1 and CA2), polypropylene (PP), ethylene-tetrafluorethylene-copolymer (E/TFE), and tetrafluorethylene-hexafluorpropylene-copolymer (F/EP) a comprehensive roughness analysis was performed. This included not only the determination of the vertical surface roughness but also the evaluation of

lateral height fluctuations and their “jaggedness”.

In addition, high-resolution AFM scans have been recorded yielding morphological information on a length scale of only a few ten nm. These measurements revealed the correlation between surface nanostructure and fabrication technique of CA. In addition to the morphological characterization, so called “phase images” were measured that allow to distinguish - at least qualitatively - between soft and hard materials. By this means the lamellae structure of E/TFE and F/EP has been analyzed. Further, for an impact-modified PMMA film with rubber inclusions of less than 100 nm diameter the method revealed the core-shell structure of the emulsion polymerized rubber inclusions.

## Experimental

The polymer films with thicknesses of 30  $\mu\text{m}$  (PP, CA1), 50  $\mu\text{m}$  (PC, CA2, E/TFE, F/EP) and 60  $\mu\text{m}$  (PMMA) were cut into disc-shaped samples with 1 cm diameter and glued on a metallic sample holder. Prior to measurement the samples have been stored at 23 °C for 24 hours at a humidity of 50 % to avoid electrostatic charging. A MultiMode™ AFM (Digital Instruments, Santa Barbara, CA, USA) with a 100  $\mu\text{m}$  x 100  $\mu\text{m}$  lateral scan range has been used. The measurements have been performed in tapping-mode™<sup>[2]</sup> under ambient conditions with sharpened Si tips (tip radius  $\leq 10$  nm, opening angle  $\approx 18^\circ$ ). In addition to topographic images, phase images<sup>[3]</sup> have been recorded representing the phase lag between the exaggerating oscillation and the detected cantilever oscillation and allowing therefore to distinguish between hard and soft sample areas.<sup>[3]</sup> The AFM images will be shown in gray-scale presentation with light corresponding to higher  $z$  values, as can be seen by comparing Fig. 1a) and Fig. 1b). The gray-scale range (shortly and hereafter called  $z$  scale) will be given with each image. Analogous, in the phase images light means smaller phase lag (i.e., soft) and dark larger phase shift (i.e., hard).

## Determination of surface roughness parameters

Due to the measurement principle of AFM<sup>[2]</sup> the resulting “image”, or better the recorded matrix  $z_{ij}$  represents a three-dimensional topography. Thus, the matrix can immediately be analyzed in terms of the root-mean square (rms) roughness  $\sigma$ :

$$\sigma = \sqrt{\frac{1}{N^2} \sum_{i=1}^N \sum_{j=1}^N [z(x_i, y_j) - \langle z \rangle]^2} . \quad (1)$$

There,  $N$  is the number of pixels in both lateral directions (here always 512) and  $\langle z \rangle$  is the average height of the image. Frequently, rough surfaces are only distinguished by their vertical roughness. For a comprehensive surface roughness characterization, however, one has also to consider the lateral fluctuations of roughness. For a random rough surface this can be quantified by the lateral correlation length  $\xi$  that denotes the average length for which the heights between two surface points are correlated. The third independent parameter to describe a rough surface is the roughness exponent  $\alpha$ , also called Hurst parameter.<sup>[4]</sup> It tells how jagged a surface with a given rms roughness and lateral correlation length is.  $\alpha$  usually ranges between 0.5 (more jagged surface) and 1 (less jagged). This set of roughness parameters can easily be determined from AFM measurements by calculating the height-height correlation function  $C(\mathbf{r})$ <sup>[4,5]</sup>

$$C(\mathbf{r}) = \langle [z(\mathbf{r}_0 + \mathbf{r}) - \langle z \rangle] [z(\mathbf{r}_0) - \langle z \rangle] \rangle . \quad (2)$$

There,  $\mathbf{r}$  denotes the lateral separation of any pairs of surface points  $\mathbf{r}_0$  and  $\mathbf{r}_0 + \mathbf{r}$  and  $\langle \dots \rangle$  means the average over all  $\mathbf{r}_0 = (x_i, y_j)$ . It can easily be seen from Eqs. (1) and (2) that  $C(0) = \sigma^2$ . For a surface that shows a self-affine fractal behavior<sup>[5]</sup> on a short length scale and that is smooth on a long length scale, the height-height correlation function can be simply written as<sup>[6]</sup>

$$C(\mathbf{r}) = \sigma^2 \exp[-(|\mathbf{r}|/\xi)^{2\alpha}] . \quad (3)$$

For  $\alpha = 0.5$  this function decays exponentially whereas it is a Gaussian for  $\alpha = 1$ . For isotropic random rough surfaces as it is the case for the films under investigation here it is sufficient to analyze the one-dimensional (1D) height-height correlation function  $C(x)$  which is simply obtained by replacing  $\mathbf{r}$  by  $x$  in Eqs. (2) and (3).<sup>[7]</sup> In Figure 1 an example is presented showing how the roughness parameters  $\sigma$ ,  $\xi$ , and  $\alpha$  can be determined from  $C(x)$ . Figures 1a) and b) show a fraction of a  $50 \mu\text{m} \times 50 \mu\text{m}$  image with a corresponding line scan  $z(x)$ , respectively. Figure 1c) represents the resulting height-height correlation function that has been averaged over all 512 line scans of the

whole image. As can be seen from Eq. (3), the lateral correlation length is characterized by the value of  $x$  at which  $C(x)$  decays to  $\sigma^2/e$ . The roughness exponent can now be determined by fitting Eq. (3) to the  $C(x)$  calculated from the AFM image. It should be noted that the same set of roughness parameters is also obtained by analyzing the height-difference function  $H(x) = \langle [z(x_0 + x) - z(x_0)]^2 \rangle$  or the Fourier transform of  $C(x)$  (also called power spectral density of roughness) in similar ways.<sup>[4]</sup> All these procedures are well established for the roughness characterization of metal and semiconductor surfaces.<sup>[4,7]</sup> Just recently they have also been successfully applied to characterize polymer film growth.<sup>[8]</sup>

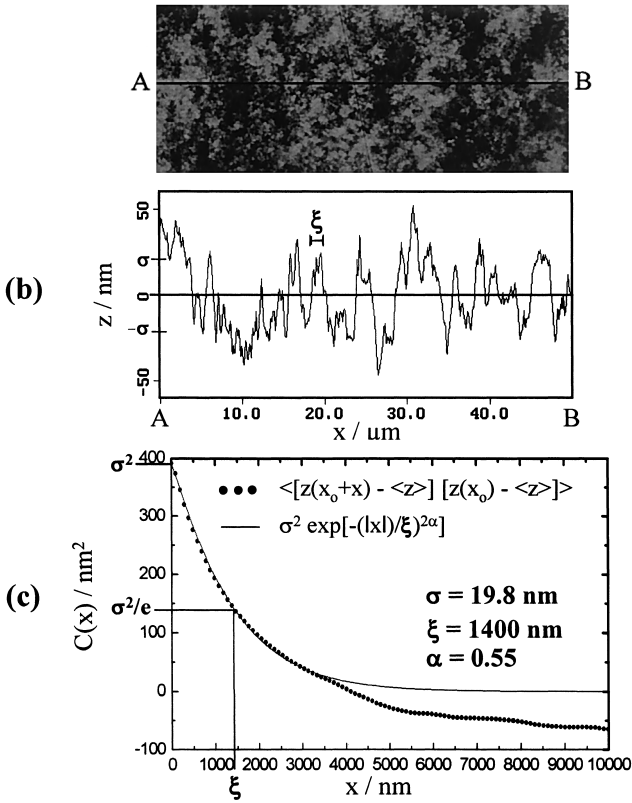


Figure 1. Example for the determination of roughness parameters for a self-affine fractal surface (in this case of a 50  $\mu\text{m}$  thick E/TFE film) from an AFM image. a) 20  $\mu\text{m}$  x 50  $\mu\text{m}$  topographic image,  $z$  scale: 120 nm. b) 1D cross-section along the line indicated in a). c) 1D height-height correlation function  $C(x)$  averaged over all scan lines and fitted curve according to Eq. (3). The rms roughness  $\sigma$  is taken as the square root from  $C(0)$  and the lateral correlation length  $\xi$  is determined by the  $1/e$  fall-off of  $C(x)$ . These quantities are also indicated in (b). The deviations for large  $x$  values are mainly due to the insufficient statistics.

## Results and discussion

### Quantitative roughness analysis

For the quantitative roughness analysis  $50\text{ }\mu\text{m} \times 50\text{ }\mu\text{m}$  AFM scans were recorded. This scan area results in a bandpass ranging from  $100\text{ nm}$  (smallest pixel distance in the images) to  $50\text{ }\mu\text{m}$  (scan size) and allows comparison with results of scattering measurements using an integrating sphere, solar-optical spectrophotometer.<sup>[1]</sup> In Figure 2, for each film a representative topographic image is presented. The images are arranged with increasing z-scale. All films with exception of CA1 exhibit a random rough surface morphology that is isotropic and therefore justifies the one-dimensional roughness analysis according to the scheme presented in Figure 1. Sample CA1 shows fiber-like structures with a preferential orientation (see below). Because these structures are superimposed on an isotropic roughness also here the 1D analysis was applied. Occasionally, there occurred contaminations or scratches on the images. Due to the large image size these do not significantly influence the roughness analysis.

The resulting roughness parameters shown in Table 1 have been averaged over five scans recorded at independent areas. The rms-roughness ranges from  $1.2\text{ nm}$  (PC) to  $35.5\text{ nm}$  (PP), thus varying over more than one order of magnitude. These values correlate quite well with the solar-optical thickness of the corresponding film.<sup>[1]</sup> The lateral correlation length is smallest for the F/EP film ( $0.4\text{ }\mu\text{m}$ ) and largest again for PP ( $2.3\text{ }\mu\text{m}$ ). Here, no correlation has been found with the solar optical thickness<sup>[1]</sup>, although there is a tendency (with exception of the F/EP film) that the lateral correlation length increases with increasing rms-roughness. The roughness exponents vary from about 0.55 (E/TFE) to 0.85 (CA2).

Table 1. Roughness parameters of transparent polymer films obtained by analysis of five independent  $50\text{ }\mu\text{m} \times 50\text{ }\mu\text{m}$  AFM images.

	rms roughness $\sigma$ (nm)	lateral correlation length $\xi$ ( $\mu\text{m}$ )	roughness exponent $\alpha$ (-)
$50\text{ }\mu\text{m}$ PC	$1.2 \pm 0.1$	$1.66 \pm 0.13$	$0.78 \pm 0.01$
$50\text{ }\mu\text{m}$ F/EP	$7.9 \pm 0.5$	$0.38 \pm 0.06$	$0.62 \pm 0.02$
$60\text{ }\mu\text{m}$ PMMA	$12.4 \pm 1.4$	$1.22 \pm 0.07$	$0.73 \pm 0.01$
$30\text{ }\mu\text{m}$ CA(1)	$13.7 \pm 1.8$	$1.00 \pm 0.19$	$0.57 \pm 0.01$
$50\text{ }\mu\text{m}$ CA(2)	$20.0 \pm 4.1$	$1.63 \pm 0.40$	$0.87 \pm 0.02$
$50\text{ }\mu\text{m}$ E/TFE	$22.6 \pm 1.2$	$1.74 \pm 0.12$	$0.57 \pm 0.02$
$30\text{ }\mu\text{m}$ PP	$35.5 \pm 2.3$	$2.32 \pm 0.16$	$0.85 \pm 0.02$

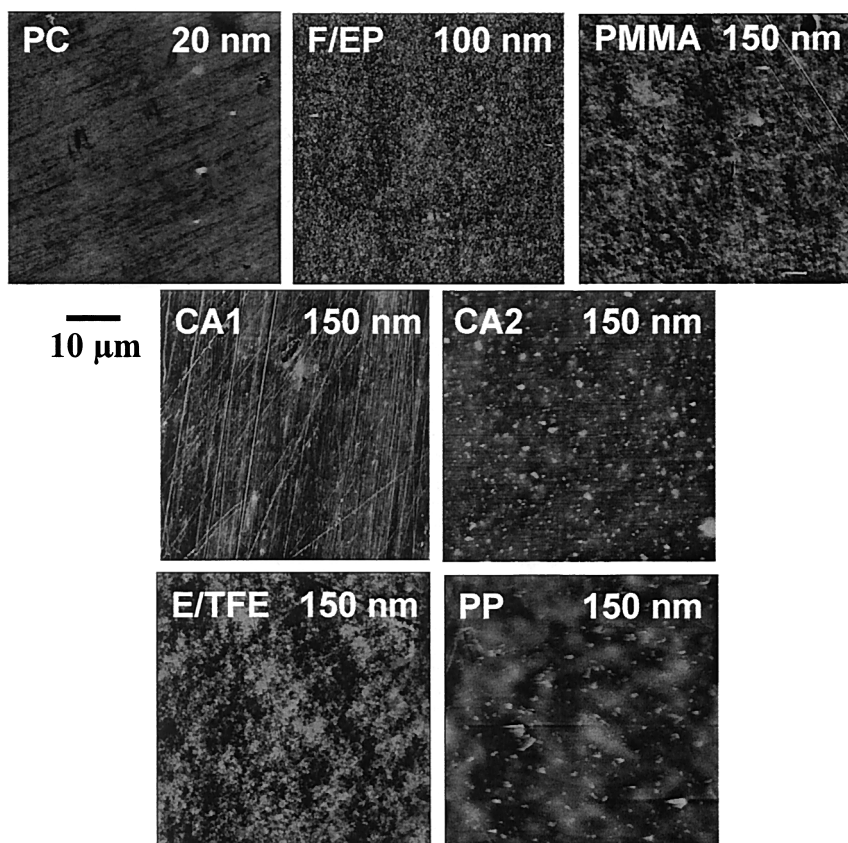


Figure 2. Series of 50  $\mu\text{m} \times 50 \mu\text{m}$  AFM images in gray-scale presentation. The corresponding value for the z-scale is given in the right corner of each image.

### Identification of nanostructures

For each of the polymer films also high-resolution AFM images with scan sizes down to at least 2  $\mu\text{m} \times 2 \mu\text{m}$  have been recorded. In the case of PP and the CA films, these images revealed the existence of nanostructures that are a consequence of the additives used and/or the manufacturing process. Figure 3 shows a 2  $\mu\text{m} \times 2 \mu\text{m}$  topography image of the PP film with a corresponding cross-section. In the center of the image a 1.3  $\mu\text{m}$  wide and about 4  $\mu\text{m}$  long plate-like structure appears like a scale. The height of this plate is about 30 nm. As one can see in the corresponding 50  $\mu\text{m} \times 50 \mu\text{m}$  image presented in Figure 2 such scales cover the entire film. Presumably, these plates can be

attributed to the fillers used. Further investigations with respect to the chemical composition of the plates might be helpful.

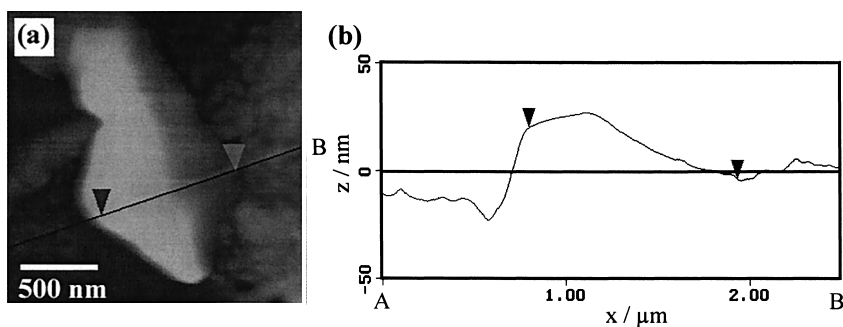


Figure 3. a)  $2\ \mu\text{m} \times 2\ \mu\text{m}$  topography image (z-scale 100 nm) of a PE covered  $30\ \mu\text{m}$  PP film. b) 1D cross-section along the line indicated in (a). The markers are shown to identify different positions on the crystalline plate.

Using high-resolution images we also analyzed the different surface features of the two CA films. The fibril-like structures visible on the CA1 film have a width of about 120 nm. Probably, they can be interpreted as the replica of the metallic casting belt that has been structured to avoid a sticking of the film after it has been rolled up. For the same reason, silicon oxide particles have been added as antiblocking agents to the CA2 film. Indeed, we found  $2\ \mu\text{m}$  lateral diameter features that stick out of the surface up to a height of about 60 nm as can be recognized already in the large-scale image in Figure 2. For the copolymers E/TFE and F/EP high-resolution topography and phase images are presented in Figure 4. Although almost invisible in the topographic images, the phase images clearly exhibit a lamellae structure for both films. The dark areas in the phase images represent the harder crystalline lamellae and the softer amorphous matrix appears bright. For E/TFE, the mean lamella width has been measured to about 60 nm and the length of the observed lamellae of about 150 nm. For F/EP both values are smaller by a factor of 2. The difference in lamellae size shows a direct correlation with the rms-roughness (see Table 1). From phase measurements on an even smaller scale that are in progress it is expected that one can determine quantitatively the area fraction of the lamellae and from that the different degree of crystallinity of both films.

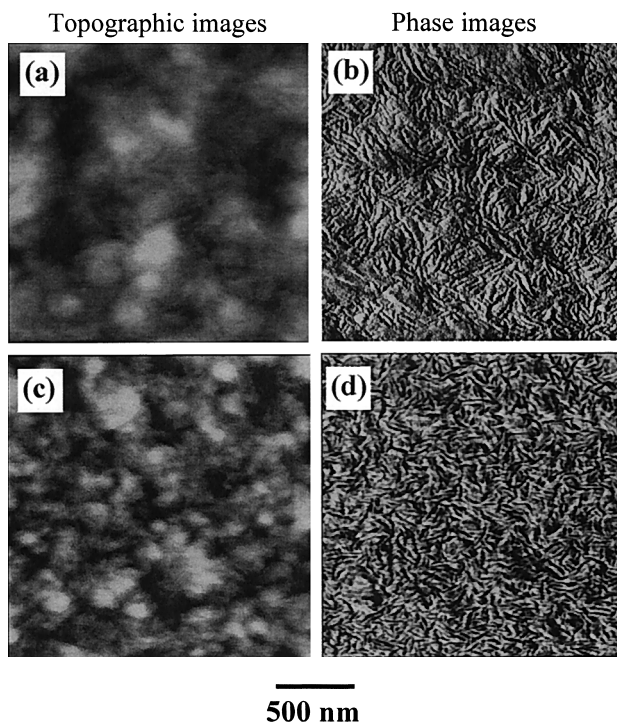


Figure 4.  $2\ \mu\text{m} \times 2\ \mu\text{m}$  topography images and corresponding phase images for E/TFE (a,b) and F/EP (c,d). z-scale 100 nm (a), 50 nm (c),  $15^\circ$  (b,d).

Finally, Figure 5 shows a detailed analysis of topography and phase images for the  $60\ \mu\text{m}$  PMMA film that has been impact modified by partly cross-linked polybutylacrylate.<sup>[9]</sup> The  $2\ \mu\text{m} \times 2\ \mu\text{m}$  topography image (Figure 5a) exhibits randomly distributed hemispheric hillocks that can be interpreted as rubber inclusions located at the surface. According to the line scan across such hillocks (see Figure 5c) their diameter is about 50 nm and their height with respect to the adjacent PMMA surface is about 10 nm. As can be seen in Figures 5 a) and c) the hillocks are surrounded by a ca. 2 nm deep trench. The corresponding phase images help to uncover the inner structure of these inclusions. In the  $2\ \mu\text{m} \times 2\ \mu\text{m}$  phase image (Figures 5b) the hillocks appear bright (independent of their height level) because they are softer than the surrounding PMMA matrix. However, the  $500\ \text{nm} \times 500\ \text{nm}$  phase image (Figures 5c) shows that the center of the inclusion is less bright than the outer parts as is clearly indicated by the ring-like features in the 3D presentation of the phase image. With other words, the



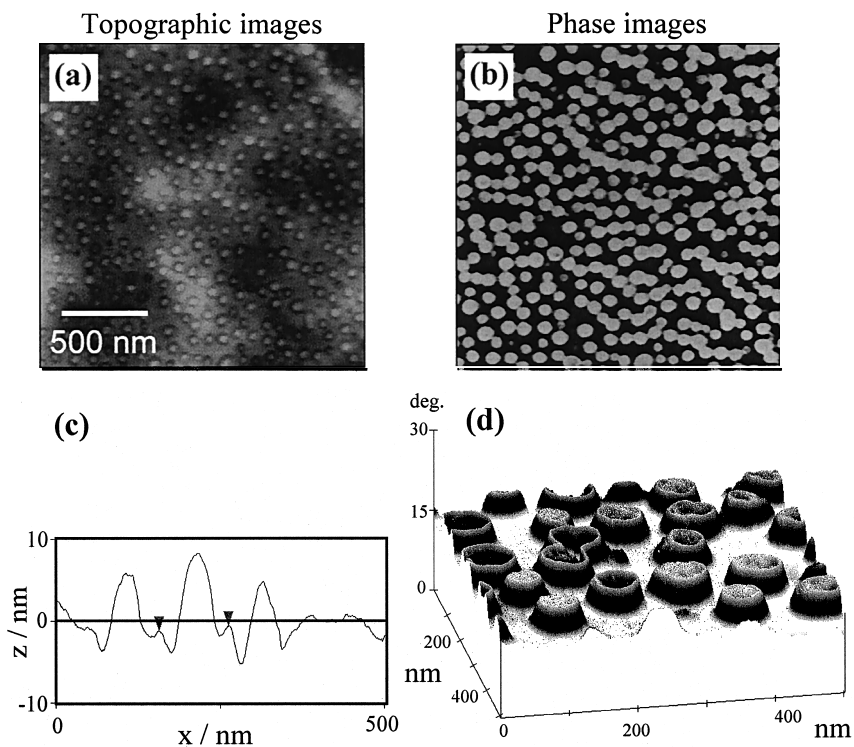


Figure 5. a,b)  $2\ \mu\text{m} \times 2\ \mu\text{m}$  topography image and corresponding phase image of an impact modified  $60\ \mu\text{m}$  PMMA film. c) 1D line scan across the hemispheric structures visible in (a). The two markers indicate the outer perimeter of the trench around each hillock. Note, that only the middle feature is cut across its center. d)  $500\ \text{nm} \times 500\ \text{nm}$  phase image in 3D presentation.

phase image resolves a core-shell structure: A hard PMMA core surrounded by a soft polybutylacrylate shell. This finding is in agreement with material specifications of the film.<sup>[9]</sup> According to the phase images, the diameter of the PMMA core is about  $50\ \text{nm}$  whereas the thickness of the polybutylacrylate shell is  $15$  to  $20\ \text{nm}$ . Thus, recording of phase images enables us to resolve the core-shell structure with a lateral resolution of about  $10\ \text{nm}$ . Comparing topography and phase images we can state that the trench in the topography corresponds to the bright (soft) ring in the phase images. This leads to the conclusion that the applied force during the measurement resulted in a significant indentation of the polybutylacrylate shell. Thus, the observed trenches in the topography images are an artefact (that is hardly avoidable when measuring compliant material with tapping mode AFM<sup>[10]</sup>). Also, it has to be noted here that a quantitative analysis of the

mechanic properties of the core-shell particles is difficult because the phase contrast depends on the indentation depth as well as on the force constant of the cantilever used.<sup>[10]</sup>

## Conclusion

For the example of highly transparent polymer films it has been demonstrated that a comprehensive analysis of surface roughness can be performed by analyzing height-height correlation functions of atomic-force microscopy images. In addition, high-resolution topographic and phase images allowed studying the correlation between material composition, manufacturing process, and surface structure of these films on the nanometer scale. For CA films, two types of surface nanostructures have been identified that have been introduced to avoid sticking together of the rolled-up films. Further, the lamellae size of E/TFE and F/EP copolymers as well as the core-shell structure of rubber inclusions of an impact modified PMMA film have been measured with a lateral resolution of about ten nm.

[1] G. M. Wallner, R. W. Lang, W. Platzer, C. Teichert, *Macromol. Symp.*, accepted.

[2] For a review on AFM see: S. N. Magonov, M.-H. Whangbo, "*Surface Analysis with STM and AFM*", VCH, Weinheim 1996.

[3] K. L. Babcock, C. B. Prater, DI Application Notes, 1995.

See also: <http://www.di.com/AppNotes/Phase/PhaseMain.html>

[4] H.-N. Yang, G.-C. Wang, T.-M. Lu, "*Diffraction from rough surfaces and dynamic Growth Fronts*" World Scientific, Singapore 1993, p. 64. Note the different use of the terms height-height correlation function and height difference function in this book and in Ref. 8.

[5] P. Meakin, "*Fractals, scaling and growth far from equilibrium*", University Press, Cambridge 1998.

[6] S. K. Sinha, E. B. Sirota, S. Garoff, H. B. Stanley, *Phys. Rev. B* **1988**, *38*, 2297.

[7] C. Teichert, J. F. MacKay, D. E. Savage, M. G. Lagally, M. Brohl, P. Wagner, *Appl. Phys. Lett.* **1995**, *66*, 2346.

[8] Y.-P. Zhao, J. B. Fortin, G. Bonvallet, G.-C. Wang, T.-M. Lu, *Phys. Rev. Lett.* **2000**, *85*, 3229.

[9] U. Numrich, Technische Folien auf Basis PMMA – Eigenschaften und Anwendungen, Firmenschrift Röhm GmbH, Darmstadt 1997.

[10] G. Bar, L. Delineau, R. Brandsch, M. Bruch, M.-H. Whangbo, *Appl. Phys. Lett.* **1999**, *75*, 4198.